ELSEVIER

Journal of Fluids and Structures 25 (2009) 654–665

JOURNAL OF FLUIDS AND STRUCTURES

www.elsevier.com/locate/jfs

Physics of temporal forcing in wakes

B. Thiria, J.E. Wesfreid

Physique et Mécanique des Milieux Hétérogènes, Ecole Supérieure de Physique et Chimie Industrielles de Paris (PMMH UMR 7636 CNRS-ESPCI-P6-P7), 10 rue Vauquelin, 75231 Paris, Cedex 5, France

Received 6 November 2008; accepted 7 April 2009

Abstract

In this paper, we review some recent results concerning the physics of forcing in open flows. First, we recall some properties of global modes in wakes, showing their shapes and their dependence on the Reynolds number and underline the importance of the mean flow correction induced by the fluctuations. Second, we show how a local temporal forcing can affect these properties, always through the modification of the mean flow, until the wake reaches a critical transition even far from the threshold. At last, we address some conjectures about an extended model suitable for describing the dynamics of forced wakes.

Keywords: Global instability; Forced wake; Mean flow correction

1. Introduction

The wake of a cylinder is one of the most well-known cases of hydrodynamical instability studies in open flows. The phenomenon is elegant and looks simple: the geometry is basic, can generally be considered as a 2-D case, and it has, in the supercritical regime, a single well-defined frequency that depends on the Reynolds number. Besides, its main properties (drag, pressure, global mode characteristics, etc.) have been covered by a large literature (experimental, numerical and theoretical). In fact, this case is commonly considered as a basic case for the understanding of more complex situations involving bluff bodies moving in a fluid. As simple as it seems, the cylinder wake, or Bénard–von Karman instability (BvK) is still one of the greatest interest for the wake community, and periodically feeds knowledges on fluid mechanics.

In particular, some recent works focused on studying bluff body wakes under forcing conditions. This issue has been highlighted by the recent increasing of studies on flow control.

By definition, the control of a flow involves an external perturbation (in time or space) which enables the changing of some of the flow characteristics in order to optimize specific values (such as drag, lift, base pressure, shear layer or vortex strength), thus naturally providing forced flows. More generally, flows under forcing conditions can be found in most of the real cases. For instance, once the structure giving rise to instability starts to vibrate itself, it acts like a temporal forcing which modifies the flow dynamics. Here again, physics of forcing can take place in all the fluid–structures interactions situations. Many studies have dealt with periodic forcing of wakes and how this forcing affect properties such as forces, structures, etc. Among these works, one can underline on the one hand, those conducted by Tokumaru and Dimotakis (1991), Dalton and Xu (2001), Protas and Wesfreid (2002) or Thiria et al. (2006) in the case of a cylinder performing rotary oscillations, many works on in-line oscillations [see extensive review

0889-9746/$ - see front matter
doi:10.1016/j.jfluidstructs.2009.04.002

by Williamson (2004)], or a combination of both, as discussed by Blackburn et al. (1999). On the other hand, even though the forcing of a wake affects properties such as forces and structure has been established, it has also been shown that the stability properties are modified depending on the forcing and that this modification is the result of a mean flow correction created by the interaction between the forcing and the global instability. This observation has been made possible through the recent result showing that linear stability theory applied on time-averaged flows can account for the behaviour of nonlinear systems [see Thiria and Wesfreid (2007), Barkley (2006), Sipp and Lebedev (2007), Mittal (2008) or Pier (2002)], involving averaged instead of basic flows to extract stability properties of any forced flows. For some cases, a well chosen forcing can even stabilize the whole wake by cancelling the absolute growth rate of the global instability. We so obtain, far for equilibrium, the basic state (Thiria and Wesfreid, 2007).

In this paper, we propose to review some of the recent results focusing on the effect of the forcing on wakes. The geometry chosen to show the effect of the forcing is simple: a two-dimensional bluff body wake (i.e. associated with a circular or triangular cylinder). We chose to present only the effect of a temporal forcing, here consisting of a sinusoidal rotation of the body itself around its axis [as in Protas and Wesfreid (2002) and Thiria et al. (2006)]. The choice of rotary oscillations has been retained because it is one of the standard temporal forcings used in flow control and is the one chosen by our group, but we assume that the physical mechanisms presented in this work can account for a large range of periodic forcings.

The present paper is structured as follows: the first part focuses on the characteristics of global modes in simple wake flow. We recall some of the important observations and theoretical considerations concerning the strong spatial inhomogeneity of the global modes, how they evolve, and their link with the modification of the mean flow above the threshold. Then, we show how a simple temporal forcing, always through modification of the mean flow, can modify the characteristics of the initial global mode until the wake reaches a critical transition even far from the threshold. Last, we address some conjectures about an extended Landau model suitable for describing the dynamics of forced wakes.

2. Spatial inhomogeneity of global modes in wake flow

2.1. Mean flow correction

For a critical control parameter, the Reynolds number (Re), the flow behind the cylinder becomes unstable and undergoes self-sustained oscillations, and the unstable basic state of the wake is modified by an observable mean flow correction. This modification is described by the nonlinear coupling of perturbations in the Navier–Stokes equation creating a non-zero stationary component induced by the wake fluctuations. This principle is illustrated in Fig. 1(a) and

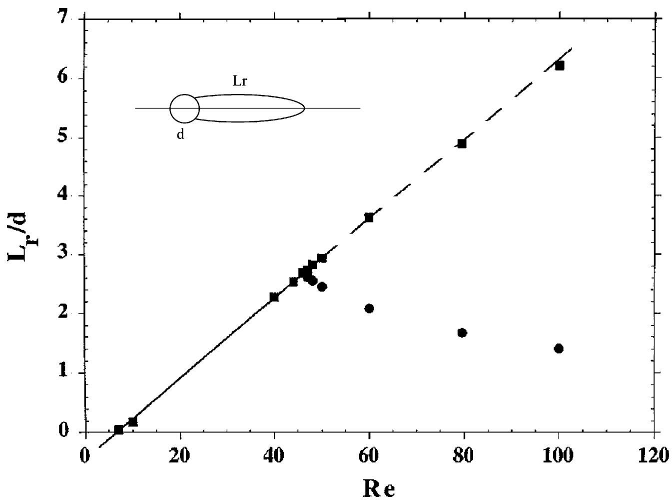

Fig. 1. Evolution of the dimensionless recirculation length L_r/d, where d is the typical length of the bluff body, as a function of the Reynolds number. Due to nonlinear effects (creation of a non-zero stationary component induced by wake fluctuations), L_r breaks up with its linear dependence in the stable branch and starts to decrease with Re (•). For a given Reynolds number, the morphology of the mean flow is then drastically far from the unsteady basic flow (◆). From Zielinska et al. (1997).

is taken from Zielinska et al. (1997). In the stable branch (below Re_c), the recirculation length, which is a footprint of the mean flow, grows linearly with Re. At the transition, L_r breaks with its linear (diffusive) dependence (represented by the dashed line from transition) and starts to decrease nonlinearly. One should note that, beyond the critical point, the wake is in an non-stationary situation and is averaged in time for comparison with the stable branch in Fig. 1. The importance of this mean flow correction appears to be crucial in the understanding of wake (forced or not) and will be discussed later.

2.2. Frequency selection

The BvK instability can be discerned by a global coherence of the oscillation. Experimentally, the relationship between Strouhal frequency of vortex shedding and the Reynolds number was established long ago by Camichel et al. (1927) and Bénard (1928), and was more recently studied by Provansal et al. (1987) and Williamson (1988), for instance. The mechanism of frequency selection of such self-sustained flows is still a challenge; from the theoretical point of view, it can be based on the analysis of the complex global local absolute frequency ω_0 which depends on the streamwise coordinate. For normal modes growing proportionally to $e^{-i(\omega_0 t - k_0 x)}$, where ω_0 and k_0 are, respectively, the complex absolute frequency and complex absolute wavenumber with zero group velocity, if $\mathrm{Im}(\omega_0) > 0$, the flow is said to be locally absolutely unstable (AU); the perturbations grow *in situ* and overrun the whole flow. On the other hand, if $\mathrm{Im}(\omega_0) < 0$, the flow is considered locally convectively unstable (CU); the perturbations are amplified but advected by the oncoming flow. It is now well known that flows giving rise to self-sustained (or global) oscillations exhibit a finite region of absolute instability which is a necessary condition for synchronization. In addition to a global study of the stability, many different criteria, based on local analysis, have been proposed: Pierrehumbert (1984), Koch (1985), Huerre and Monkewitz (1990), Chomaz et al. (1991) and others [see Chomaz (2005) for a review]. Even though some works have already used time-averaged flow with stability theory [see for instance Mattingly and Criminale (1972), Triantaffylou et al. (1986) or Hammond and Redekopp (1997)], it has finally been found that the first stability analysis that can account for the observed selected frequency in spatially developed open flows, even far from the onset, is a linear theory applied on the time-averaged flow, instead of the unperturbed basic flow. Results showing that singularity have been presented for the first time by Pier (2002) (see Fig. 2). Later, Barkley (2006), Sipp and Lebedev (2007) and

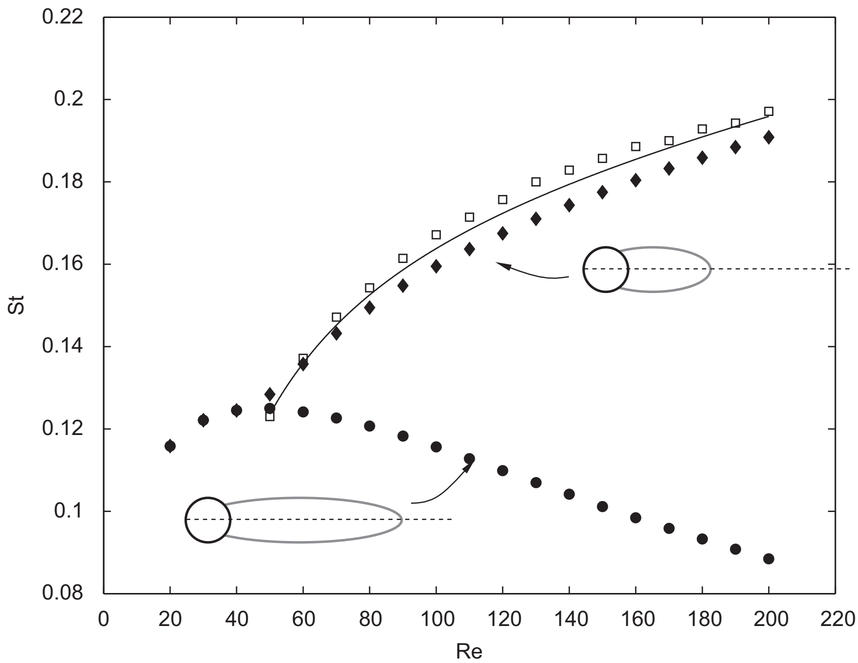

Fig. 2. Evolution of the global selected frequency in the wake of a circular cylinder as a function of the Reynolds number: □, frequency obtained by direct numerical simulation (DNS); —, experimental results from Williamson (1988). Results (ω_s), represented by (◆), have been obtained by applying the linear saddle-point criterion x_s [see Chomaz et al. (1991)] on the time-averaged mean flow. The (•) represent the same calculation applied on the unperturbed basic flow. From Pier (2002).

Mittal (2008) have advanced some theoretical conjectures showing that the mean state corresponds to a marginally stable situation and that the eigenfrequencies associated with the global modes follow the experimental curve for quite a large range of Reynolds numbers above the threshold. In addition, Thiria et al. (2008) showed that, even in the transient regime, the instantaneous selected frequency (and more generally the stability properties), are entirely determined by the mean state at this instance.

2.3. Global mode envelope

In the mid-nineties, some works have focused on the scaling laws of the spatial shape of the global mode (i.e. envelope of the peak-to-peak amplitude of fluctuations), previous works on the formation length consisting only in qualitative discussion about the spatial behaviour. Goujon-Durand et al. (1994), Wesfreid and Zielinska (1995) and then Wesfreid et al. (1996) have been among the first to point out the spatial inhomogeneity of the selected modes as an extension of previous works in confined instabilities as the Rayleigh–Bénard convection [see Wesfreid et al. (1978)]. In Fig. 3, we show the typical structure of the global mode for a given supercritical Reynolds number (here $\mathrm{Re} = 1.213\mathrm{Re}_c$). As shown, the distribution of fluctuations is strongly inhomogeneous (non-parallel) and presents two symmetric clear maxima close to the body. For more clarity, one can have a look to Fig. 3(b) which is taken from Wesfreid and Zielinska (1995), and displays the global mode shape as the only coordinate x (i.e. for fixed abscissa coordinate y). This is the classical representation of the envelope of the global mode. It has a sharp front, a maximum $a_{\max}$ corresponding to its spatial position $x_{\max}$ and then diffuses far from the body to the streamwise stable region. The study displayed in Fig. 3(b) has focused on the evolution of this shape as a function of the Reynolds in the supercritical regime. They proposed that both $a_{\max}$ and $x_{\max}$ follow scaling laws of the following form:

$$a_{\max} \simeq (\mathrm{Re} - \mathrm{Re}_c)^{1/2}, \quad x_{\max} \simeq (\mathrm{Re} - \mathrm{Re}_c)^{-1/2}, \tag{1}$$

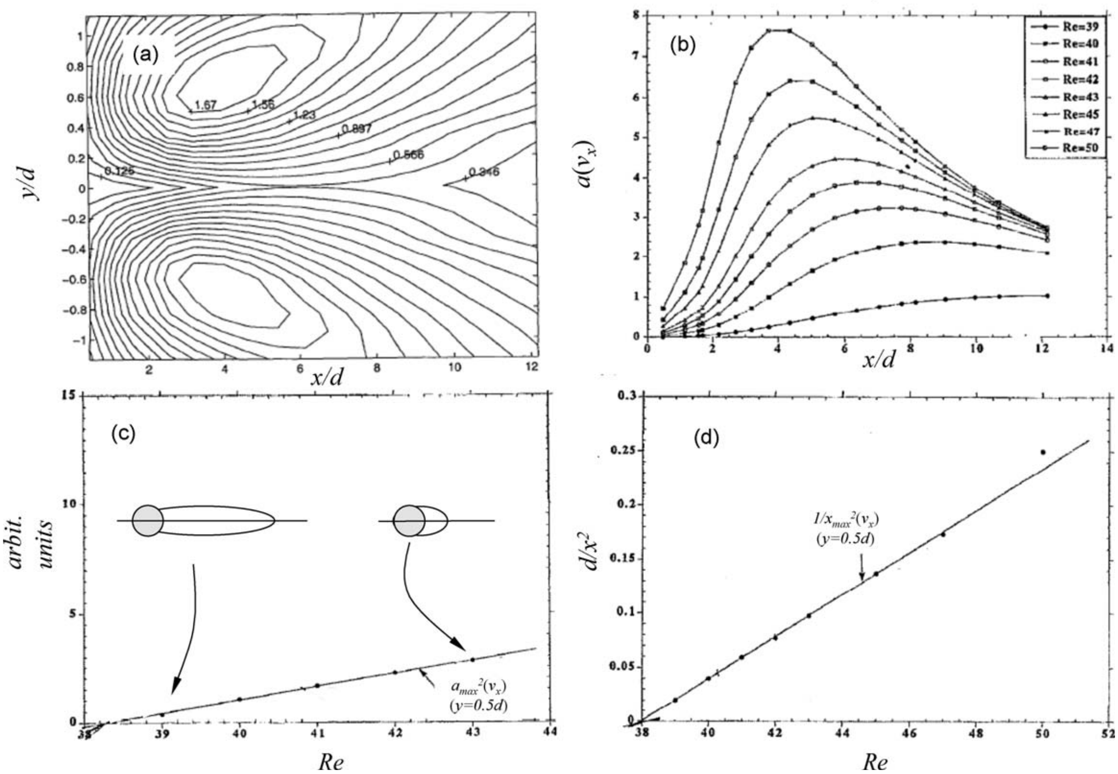

Fig. 3. (a) Isocontours of the fluctuating velocity modulus for the streamwise fluctuation v_x (2-D global mode shape) in the x–y plane. The flow is from left to right and the bluff body is located at coordinates ($x/d = 0$, $y/d = 0$). (b) One-dimensional representation of the global mode shape (streamwise evolution for a fixed y/d) as a function of the Reynolds number. (c) and (d) Linear dependence of the square of maximum of the fluctuation $a^2_{\max}$ and the inverse of the square of the typical lengthscale $1/x^2_{\max}$ showing that global modes follow scaling laws. (a) From Wesfreid et al. (1996); (b)–(d) from Wesfreid and Zielinska (1995) for a triangular cylinder.

where Re_c is the critical Reynolds number corresponding to the onset of the instability. Those scaling laws have been confirmed using a simplified Ginzburg–Landau model [see Couairon and Chomaz (1999)]. Sufficiently close to the threshold, this model, simple though it is, gives a good representation of the dynamics for such nonlinear flows. It is also important to notice that scaling laws derived from a Landau model do not exist in the whole instability domain and describe the critical behaviour close to the onset of instability. As inhomogeneities are important in such systems (due to the relaxation of the shear profile with advection), there is a competition between purely nonlinear effects and spatial inhomogeneity. Thus, if $x_{\max}$ is located in the region of absolute instability, where nonlinear effects dominate, a dynamic front takes place as it evolves in an homogeneous medium. $x_{\max}$ can be assimilated to the correlation length and scales as $(\mathrm{Re} - \mathrm{Re}_c)^{-1/2}$ as shown in Fig. 3. Besides, and that is the case far from the threshold, if $x_{\max}$ is outside the region of absolute instability, inhomogeneities prevail, the model used cannot account for the evolution of the global mode shape [see detailed discussions in Couairon and Chomaz (1999) or Goujon-Durand and Wesfreid (2005) and same remarks can be made about $a_{\max}$]. Those observations will be discussed again later, in the case of a forced wake.

3. Dynamics of forced wakes

In the following, the modifications of the general properties observed in free wakes, when they are subjected to periodical temporal forcing, are discussed. As introduced above, we chose to consider a classical temporal forcing in the wake that consists of performing rotary oscillations of the cylinder itself, as displayed in Fig. 4. We define a forcing amplitude A that is the ratio between the maximal azimuthal velocity and the upstream velocity u_∞ and a forcing frequency f_f. We also introduce the frequency f_0 which corresponds to the natural shedding frequency without forcing. We present results performed at $\mathrm{Re} = 150$. Most of the time, we chose to focus on one single forcing frequency, $f_f = 5f_0$, and to study the evolution of the wake as a function of A. This choice has been made in this framework, because that particular forcing frequency is one where a wide range of changes can be observed with respect to the forcing amplitude, so that we can get details on the dynamics. Other frequencies have been treated in Thiria et al. (2006) and Thiria and Wesfreid (2007), and the physical behaviour is similar. Previous works have shown that, even for small external perturbations, the wake structure was strongly modified. Fig. 5, from Thiria et al. (2006), shows the evolution of a cylinder wake structure at $\mathrm{Re} = 150$ subjected to rotating oscillations of the body itself as a function of the forcing amplitude. This dynamic has been observed for different types of temporal forcing [in-line, cross-line oscillations, rotary oscillations, etc.; see for example Protas and Wesfreid (2002), Willden (2002), Nishihara et al. (2005) or Bergmann et al. (2005)].

As can be seen in Fig. 5, the forcing vortices are shed at the forcing frequency in the near-wake for a typical lock-in length depending on the forcing parameters, but merge downstream from both rows to give a new pattern similar to the one observed in the unforced case. Quantitatively, one of the features of this new dynamic is the strong mean flow correction created this time by the forcing. This phenomenon is clearly shown in Fig. 6. for the same forcing parameters as in Fig. 5. The recirculation length (blue region), initially about $2d$ can be extended to $8 - 10d$, depending on the forcing conditions.

Thiria and Wesfreid (2007) showed that vortices corresponding to the lock-in region had no clear dynamics as Kármán vortices and diffused very quickly in the wake. Besides, the far wake dynamics has been found to be more complex. After performing a complete local linear stability analysis using the Rayleigh equation solved numerically,

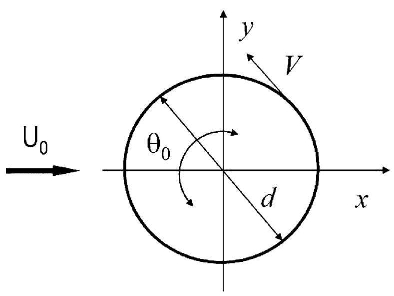

Fig. 4. Description of the oscillating motion.

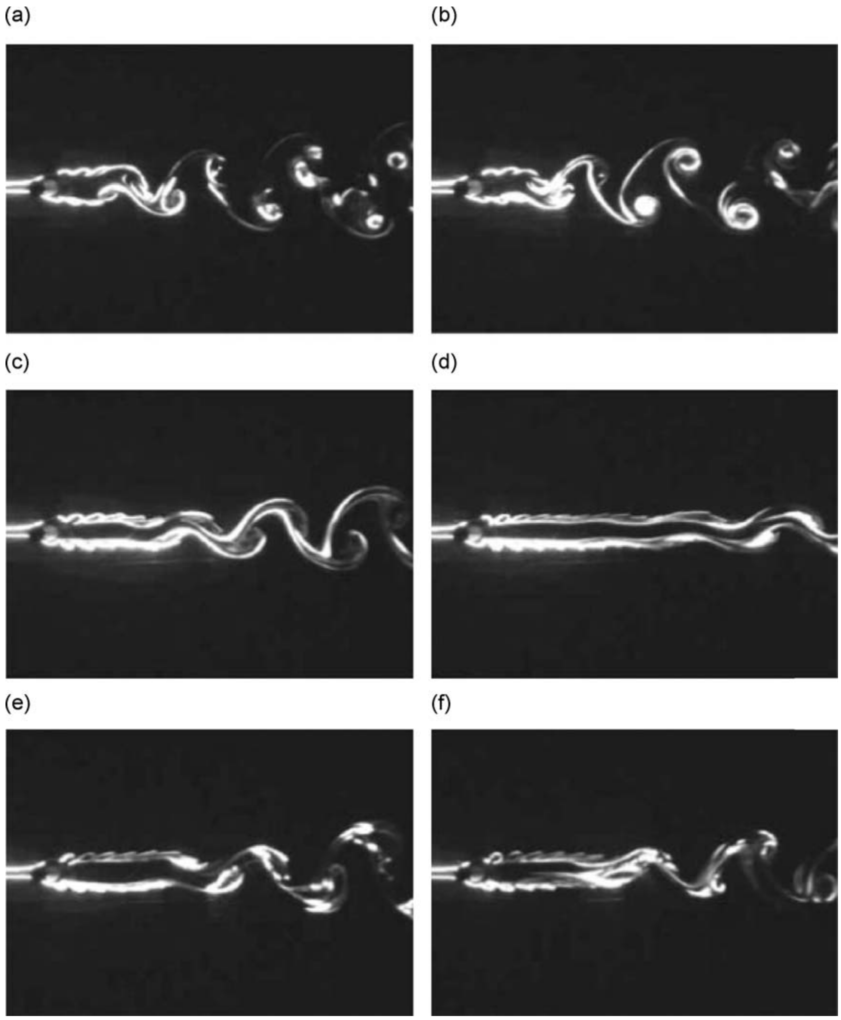

Fig. 5. Effect of the forcing on the wake structure (here the frequency is fixed and the amplitude A varies). The forcing frequency is $f_f/f_0 = 5$, the forcing amplitude is (a) $A = 1$, (b) $A = 2$, (c) $A = 4$, (d) $A = 5$, (e) $A = 7$ and (f) $A = 9$.

based on the averaged forced flows obtained *experimentally*, they found that the far-wake dynamics under forcing conditions was a new global mode selected by the system: the frequency, but also the absolute growth rate (and so its spatial shape), are different from those selected in free case, due to the modifications of the mean properties that change the intensity and the length of the absolute region. The distribution of local absolute pulsation and absolute growth rate as well as the critical transition between absolute and convective zone are drastically different and are determined by the forcing parameters. Moreover, for some parameters, the forcing is able to completely avoid the global instability (as can be seen on the left inlet of Fig. 7) to give a globally stable flow. By applying this stability analysis to a sufficient number of forcing cases, they have been able to draw the first stability diagram for the forced wake. This result, from Thiria and Wesfreid (2007), is displayed in Fig. 7. The thick lines, in the A versus f_f/f_0 plane, correspond to the critical limits where transition from global instability to global stability occurs. Those critical lines of course depend on the nature of the forcing and the body, and diagrams for in-line oscillation or a square-cylinder wake should not be the same. However, we assume once again that the physics of these phenomena remain the same [some recent studies performed on a partially masked cylinder, as suggested in Bergmann et al. (2006), have already given some confirmation to this conjecture (Godoy-Diana et al., 2008)].

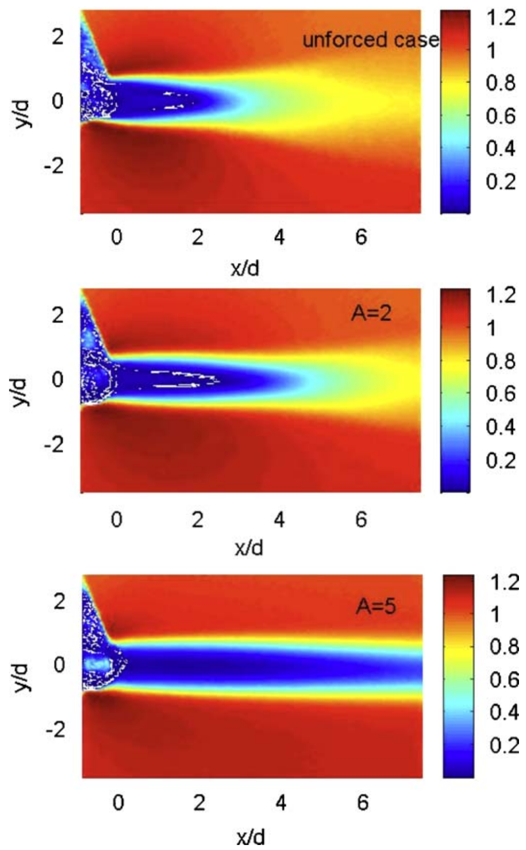

Fig. 6. Time-averaged flows obtained by PIV for different forcing amplitude at forcing frequency $f_f/f_0 = 5$, showing the strong modification induced by cylinder oscillations. The blue zone on the top left of the cylinder corresponds to the shadow of the laser sheet and has no physical meaning.

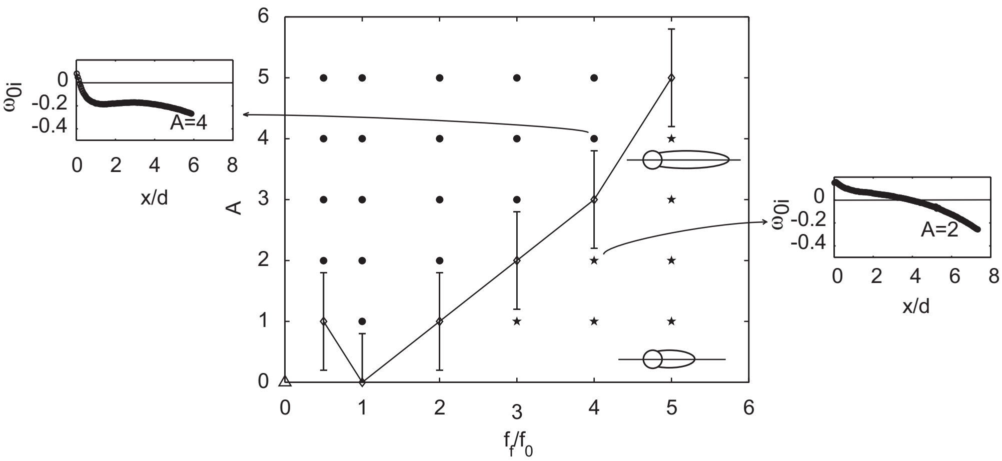

Fig. 7. Predicted global stability properties of forced wakes in the $A{-}f_f/f_0$ plane. The symbols (•) denote a globally stable flow, while the symbols (⋆) denote a globally unstable flow. The lozenges (◇) indicate the transition between these two states, corresponding to a critical value of the forcing amplitude A_c, for each forcing frequency. The two insets correspond to the spatial evolution of the absolute growth rate for two characteristic cases (globally unstable and globally stable): $f_f/f_0 = 4,\ A = 2$ (right) and $f_f/f_0 = 4,\ A = 4$ (left). As can be seen, the absolute region disappears by crossing the critical line, giving a globally stable flow.

3.1. Forced global modes

As we have seen that a transition from a globally unstable to a globally unstable flow can occur even far from the threshold through the action of the forcing, we performed, in another work (Thiria et al., 2009), a detailed study following the evolution of those selected modes from the free case to the critical line shown in Fig. 7. This study has been made using a numerical simulation with spectral methods [the same as used in Wesfreid and Zielinska (1995)] for the same parameters as Thiria et al. (2006) and Thiria and Wesfreid (2007), with the forcing frequency still set to $5f_0$.

Fig. 8 shows the evolution of the global mode shape as a function of the forcing amplitude A. As can be seen, the global instability (characterized by its front and amplitude) is pushed back downstream as we approach the critical line displayed in Fig. 7. The last global mode to be displayed corresponds to a forcing amplitude $A = 3.85$. For greater amplitudes, the position of the front and amplitude were outside of our field, but we assume that they exist until the global stabilization of the wake for $A{\sim}5$. This first observation recalls what we have seen for free wakes and which is displayed in Fig. 3(b). Fig. 8(b) shows the corresponding selected global frequency as a function of A. As already noticed in Thiria and Wesfreid (2007), the Strouhal number $\mathrm{St} = u_\infty f/d$ decreases from the natural selected frequency $\mathrm{St} = 0.185$ without forcing to $\mathrm{St} = 0.115$ as the wake stabilizes. One important remark is that the last selected

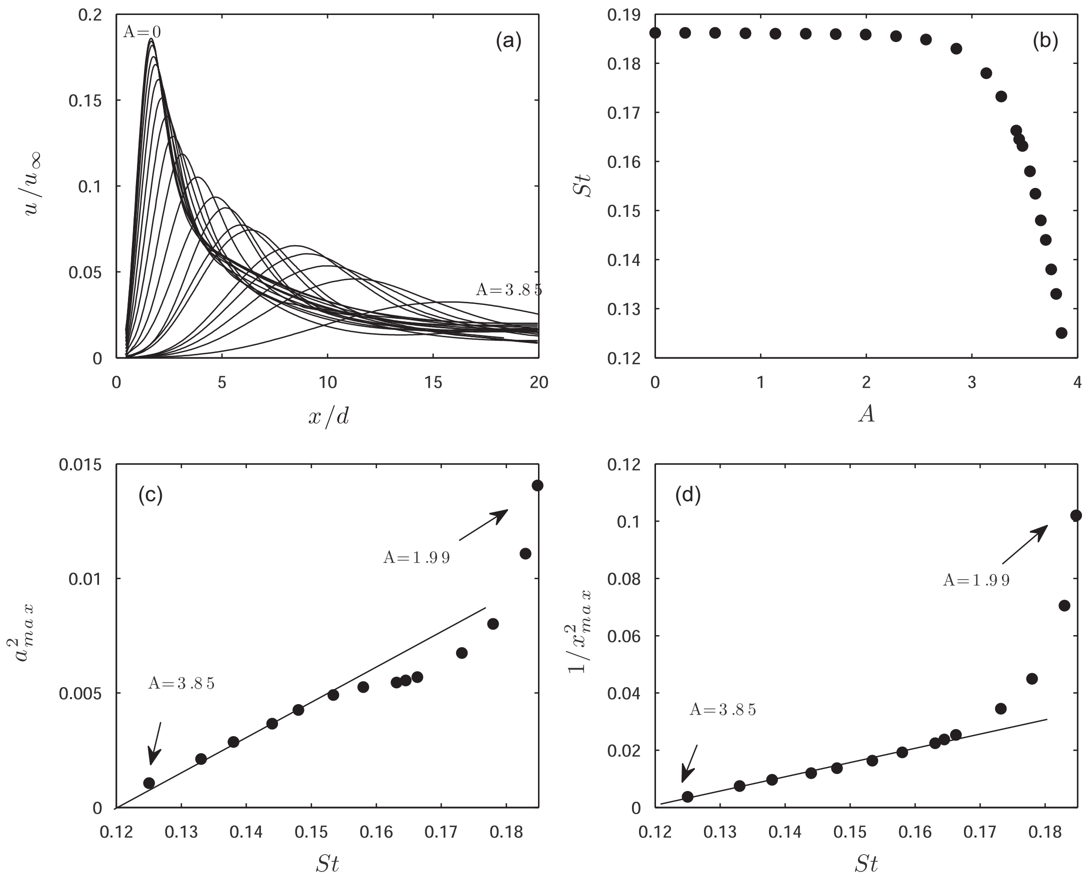

Fig. 8. (a) Evolution of the global mode shape as a function of the forcing amplitude. Measurements have been taken at the same crosswise coordinate y/d as Fig. 3 along the streamwise direction. As can be seen, global instability is pushed back downstream until a global stabilization of the wake. (b) Corresponding selected Strouhal number ($\mathrm{St} = u_\infty f/d$) as a function of A. The global frequency decreases from $\mathrm{St}_0 = 0.185$, which corresponds to the natural global frequency, to $\mathrm{St} = 0.115$, which is close to the linear global frequency selected by the basic flow. (c) and (d) Linear dependence of the square of maximum of the fluctuation $a^2_{\max}$ and the inverse of the square of the typical lengthscale $1/x^2_{\max}$ as a function of St, showing that forced global modes also follow scaling laws close to the critical lines of Fig. 7. From Thiria et al. (2009).

frequency, which can be defined as a threshold frequency (say $\mathrm{St}_0 = 0.115$) is very close to the frequency linearly selected on the basic flow (see Fig. 2). Moreover, one can note that the first frequency is numerically observed while the second is a theoretical prediction based on the saddle-point criterion, strengthening the fact that both values are nearly the same. As to knowing whether forced global modes have scaling laws too, we then have to choose a control parameter. If forced wakes follow a Landau model, we should expect that the global frequency evolves, as for nonlinear oscillators, as the square of the amplitude of the perturbation. Figs. 8(c) and (d) display the evolution of $a^2_{\max}$ and $1/x^2_{\max}$ with the corresponding selected Strouhal number. We indeed observe that both quantities scale like St, which means that they follow scaling laws of the form: $a_{\max}{\sim}(\mathrm{St}-\mathrm{St}_0)^{1/2}$ and $x_{\max}{\sim}(\mathrm{St}-\mathrm{St}_0)^{-1/2}$. As discussed in the previous section, when the case considered is far from the critical line, strong inhomogeneities in the wake should prevail upon nonlinear effects, changing the evolution of these critical parameters. However, scaling laws exist for a quite large domain from the transition AU/CU. Even far from the onset of instability ($\mathrm{Re} = 150 > 3\mathrm{Re}_c$), this thus shows that a single temporal forcing can lead to classical critical behaviour.

4. Discussion and conclusion

We have showed that an external forcing can modify the intrinsic dynamics of the wake by selecting a new global mode. This happens through the modification of the mean flow that contains stability properties as has recently been shown. Depending on the forcing parameters, a transition from a global unstable to a global stable flow can occur. Coming up to this threshold, we have seen that the forced global modes followed critical behaviours as other instabilities described by nonlinear simplified models. Finally, it appears that the selection of a global mode for flow under forcing conditions is of the same kind as those selected in the natural case. For greater clarity, this principle is illustrated in Fig. 9. The length of the reverse-flow region L_r, which is the footprint of the mean state, is plotted as a function of the Reynolds number. In the classic case of the flow behind an obstacle, which can be followed from left to right in Fig. 9, L_r grows linearly with Re in the stable region, located on the left of Re_c. When $\mathrm{Re} > \mathrm{Re}_c$, the flow becomes unstable, L_r decreases as a consequence of the mean flow modification, and a global mode is selected. Its frequency is then linearly determined by its mean state and its spatial properties are dictated by the scaling laws given in the previous section. Under forcing conditions, the mean flow is corrected, the new state selects a new mode and the bifurcation then can be seen from up to down. The different forced states with global instability (or no-lock-on state) are distributed on a vertical line (for $\mathrm{Re} > \mathrm{Re}_c$). Recently, we have shown that the same relation between the selected global frequency and wake recirculation region under blockage condition were closely linked, involving that the

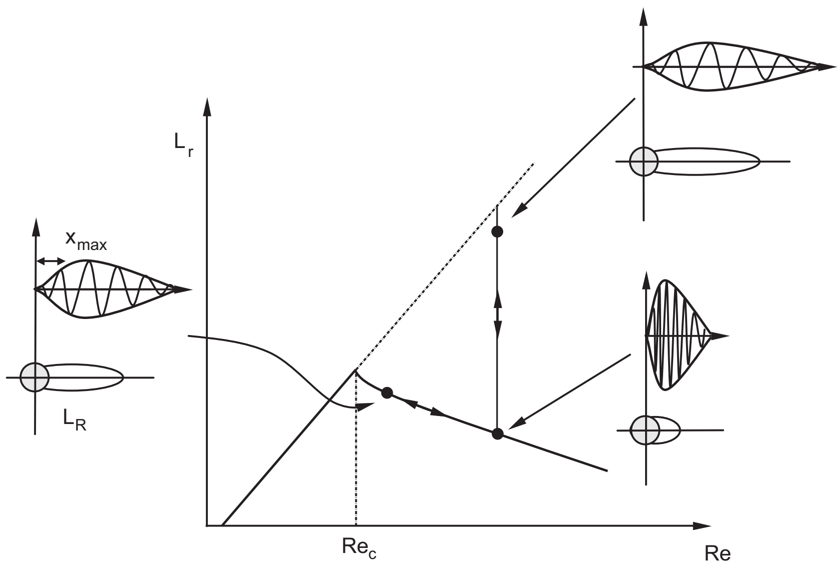

Fig. 9. Schematic view of the possible bifurcations that can occur for a cylinder under temporal forcing conditions. The vertical line, for $\mathrm{Re} > \mathrm{Re}_c$, is explored when the forcing A goes from 0 (lower branch) to the critical value given by the critical line given in Fig. 7 when the wake reaches its basic state. From Thiria and Wesfreid (2007).

dynamics such as described above could account for a wide range of forcing [see Patil and Tiwari (2008); same behaviours can be observed in the wake visualizations of a cylinder controlled by a "slip" splitter-plate obtained by Mittal (2003)].

Amplitude equations such as the Ginzburg–Landau[1] or Stuart–Landau models which give a good description of the wake dynamics near the threshold could be extended to forced wakes by taking into account the mean flow correction induced by the forcing. Corrections towards those models had already been studied in other physical situations, such as the Rayleigh–Bénard instability [see Siggia and Zippelius (1981) and Zippelius and Siggia (1983); a coupled term in the Ginzburg–Landau equation is introduced to account for an additional stationary mode]. Thus, in order to integrate the modification of the global dynamic due to this forcing, a system of coupled equations can be written as follows:

$$\begin{cases} \tau_0 \dfrac{da}{dt} = \varepsilon(1 + \mathrm{i}c_0)a - g(1 + \mathrm{i}c_1)|a|^2 a + \gamma(1 + \mathrm{i}\beta)ab, \\ \tau_1 \dfrac{db}{dt} = -\sigma b + F(A, f_f), \end{cases} \tag{2}$$

where a is here the complex amplitude of the perturbation and c_0, c_1, g, γ, β, σ, τ_0 and τ_1 are real coefficients. The equation for b is that of the quadratic mean flow correction generated by the forcing, here depending on the forcing parameters. This equation is coupled to those used for the free wake [see for instance Provansal et al. (1987)]: a new term $(\beta_r + \mathrm{i}\beta_i)ab$ appears, modifying the linear growth rate. Such a system could, *a priori*, account for the wake dynamics of a cylinder performing rotary oscillation, which is consistent with our experimental results, and more generally for many forced open flows. For instance, this approach is close to those adopted by Schumm et al. (1994) who studied the validity of the Stuart–Landau model in the transient regime between controlled and non-controlled wakes (once the control is turned off). Their study did not include an extra term corresponding to the forcing, suggesting that the total global dynamics is contained in a single equation whether or not the flow is forced.

However, we believe that the presence of this extra term is important to describe the mechanisms that are involved in the dynamics of forcing. If a simple Stuart–Landau model is sufficient, all the states located on the critical line of Fig. 7 should then be well described by a linear equation, that is $da/dt = \varepsilon(1 + \mathrm{i}c_0)a$. On the one hand, this relation should fail to give the right frequency at the transition; the above relation shows that St_c increases with Re, which is not the case according to Pier (2002) or Barkley (2006). On the other hand, far from the classical threshold (for instance $\mathrm{Re} = 150 > 3\mathrm{Re}_c$ in our case), the recirculation length of the basic state is about 4 times the one observed for Re_c, making these two flows drastically different, and we do not know, at the moment, if both dynamics (from Re_c to $\mathrm{Re} = 150$ *with no forcing*, and from $\mathrm{Re} = 150$ *with forcing* to $\mathrm{Re} = 150$ *with no forcing*, see Fig. 9) are exactly the same. In contrast, the introduction of the new term in ab should be able to fill some of these lacunae. For instance, as b is maximum on the critical line (maximum of the mean flow correction due to the forcing that leads to the GU/GS transition), the linear regime then would become $da/dt = \varepsilon(1 + \mathrm{i}c_0)a + \gamma(1 + \mathrm{i}\beta)ab$ and would allow to retrieve the correct dynamics at the onset. Similar arguments can be put forward in the nonlinear regime and we are now working on experiments that could precisely detail the validity of this model, especially by analysing the behaviour of $|a|^2$ (determination of the Landau constant) as a function of the Reynolds number *and* the forcing parameters. This study confirms that controlled, and more generally forced wakes, do have nonlinear critical behaviour, whatever the nature of the control.

Acknowledgements

The authors are grateful to G. Bouchet, who contributed to a large part of the numerical work. We also thank Sophie Goujon-Durand, Patrice Jenffer and Daniel Pradal for their contribution to the experimental set-up.

References

Bénard, H., 1928. Sur les tourbillons alternés et la loi de similitude. Comptes-Rendus de l'Académie des Sciences 187, 1123–1125.

Blackburn, H., Elston, J., Sheridan, J., 1999. Bluff-body propulsion produced by combined rotary and translational oscillation. Physics of Fluids 11, 4–6.

[1]In the following, the Landau amplitude equation is sufficient, without the Ginzburg terms corresponding to spatial inhomogeneities.

Barkley, D., 2006. Linear analysis of the cylinder in wake mean flow. Europhysics Letters 75, 750–756.

Bergmann, M., Cordier, L., Brancher, J.-P., 2005. Optimal rotary control of the cylinder wake using proper orthogonal decomposition reduced-order model. Physics of Fluids 17, 1–21.

Bergmann, M., Cordier, L., Brancher, J.-P., 2006. On the generation of a reverse von Karman street for the controlled cylinder wake in the laminar regime. Physics of Fluids 18, 1–4.

Camichel, C., Dupin, P., Tessier-Solier, M., 1927. Sur l'application de la loi de similitude aux périodes de formation des tourbillons alternés de Bénard-Karman. Comptes-Rendus de l'Académie des Sciences 185, 1556–1559.

Chomaz, J.-M., Huerre, P., Redekopp, L., 1991. A frequency selection criterion in spatially developing flows. Studies in Applied Mathematics 84, 119–144.

Chomaz, J.-M., 2005. Global instabilities in spatially developing flows. Annual Review of Fluid Mechanics 37, 357–392.

Couairon, A., Chomaz, J.-M., 1999. Fully nonlinear global modes in slowly varying flows. Physics of Fluids 11, 810–826.

Dalton, C., Xu, Y., 2001. The suppression of lift on a circular cylinder due to vortex shedding at moderate Reynolds numbers. Journal of Fluids and Structures 15, 617–628.

Godoy-Diana, R., Duriez, T., Wesfreid, J.E., 2008. Private communication.

Goujon-Durand, S., Jenffer, P., Wesfreid, J.E., 1994. Downstream evolution of the Bénard von Kármán instability. Physical Review E 50, 308–313.

Goujon-Durand, S., Wesfreid, J.E., 2005. Spatial inhomogeneities in hydrodynamic instabilities. In: Mutabazi, I., Wesfreid, J.E., Guyon, E. (Eds.), Dynamics of Spatio-temporal Cellular Structures: Henri Bénard Centenary Review. Springer, Berlin, pp. 203–210.

Hammond, D., Redekopp, L., 1997. Global dynamics of symmetric and asymmetric wakes. Journal of Fluid Mechanics 331, 231–260.

Huerre, P., Monkewitz, P.A., 1990. Local and global instabilities in spatially developing flows. Annual Review of Fluid Mechanics 22, 473–537.

Koch, W., 1985. Local instability characteristics and frequency determination on self-excited wake flows. Journal of Sound and Vibrations 99, 53–83.

Mattingly, G., Criminale, W., 1972. The stability of an incompressible two-dimensional wake. Journal of Fluid Mechanics 58, 111–118.

Mittal, S., 2003. Effect of a "slip" splitter plate on vortex shedding from a cylinder. Physics of Fluids 15, 817–820.

Mittal, S., 2008. Global linear stability analysis of time-averaged flows. International Journal for Numerical Methods in Fluids 51, 233–272.

Nishihara, T., Kanedo, S., Watanabe, T., 2005. Characteristics of fluid dynamic forces acting on a circular cylinder oscillating in the streamwise direction and its wake pattern. Journal of Fluids and Structures 13, 551–578.

Patil, P., Tiwari, S., 2008. Effect of blockage on wake transition for flow past square cylinder. Fluid Dynamics Research 40, 753–778.

Pier, B., 2002. On the frequency selection of finite-amplitude vortex shedding in the cylinder wake. Journal of Fluid Mechanics 579, 137–161.

Pierrehumbert, R., 1984. Local and global baroclinic instability of zonally varying flow. Journal of the Atmospheric Sciences 41, 2141–2162.

Provansal, M., Mathis, C., Boyer, L., 1987. Bénard–Von Karman instability: transient and forced regimes. Journal of Fluid Mechanics 182, 1–22.

Protas, B., Wesfreid, J.E., 2002. Optimal rotary control of the cylinder wake in the laminar regime. Physics of Fluids 14, 810–826.

Schumm, M., Berger, E., Monkewitz, P.A., 1994. Self-excited oscillations in the wake of two-dimensional bluff bodies and their control. Journal of Fluid Mechanics 271, 17–53.

Siggia, E., Zippelius, A., 1981. Pattern selection in Rayleigh–Bénard convection. Physics of Fluids 26, 2905–2915.

Sipp, D., Lebedev, A., 2007. Global stability of base and mean flows: a general approach and its applications to cylinder and open cavity flows. Journal of Fluid Mechanics 593, 333–358.

Thiria, B., Goujoun-Durand, S., Wesfreid, J.E., 2006. The wake of a cylinder performing rotary oscillations. Journal of Fluid Mechanics 458, 407–417.

Thiria, B., Wesfreid, J.E., 2007. Stability properties of forced wakes. Journal of Fluid Mechanics 579, 137–161.

Thiria, B., Bouchet, G., Wesfreid, J.E., 2008. On the relation between linear stability analysis and mean flow properties in wakes. European Journal of Mechanics B/Fluids, submitted for publication.

Thiria, B., Bouchet, G., Wesfreid, J.E., 2009. Critical properties of forced wakes. Physical Review Letters, submitted for publication.

Tokumaru, P., Dimotakis, C., 1991. Rotary oscillation control of a cylinder wake. Journal of Fluid Mechanics 224, 77–90.

Triantaffylou, G.S., Triantaffylou, M.S., Chryssostomidis, C., 1986. On the formation of vortex streets behind stationary cylinders. Journal of Fluid Mechanics 170, 461–477.

Williamson, C.H.K., 1988. Defining a universal and continuous Strouhal–Reynolds number relationship for the laminar vortex shedding of a circular cylinder. Physics of Fluids 31, 2742–2744.

Wesfreid, J.E., Pomeau, Y., Dubois, M., Normand, C., Bergé, P., 1978. Critical effects in Rayleigh Bénard convection. Journal de Physique France 39, 725.

Wesfreid, J.E., Zielinska, B., 1995. On the spatial structure of global modes in wake flow. Physics of Fluids 7, 1418–1424.

Wesfreid, J.E., Goujon-Durand, S., Zielinska, B.J.A., 1996. Global mode behavior of the streamwise velocity in wakes. Journal de Physique Paris II 6, 1343–1357.

Willden, R.H.J., 2002. Numerical prediction of VIV on long flexible circular cylinder. Journal of Fluids and Structures 15, 659–669.
Williamson, C.H.K., 2004. Vortex induced vibrations. Annual Review of Fluid Mechanics 36, 413–455.
Zielinska, B.J.A., Goujon-Durand, S., Dusek, J., Wesfreid, J.E., 1997. Strongly nonlinear effect in unstable wakes. Physical Review Letters 79, 3688–3703.
Zippelius, A., Siggia, E., 1983. Stability of finite amplitude convection. Physical Review Letters 47, 835–838.